

# WAVES IN PRESENCE OF SHEAR CURRENT WITH UNIFORM VORTICITY

YAN LI<sup>1</sup> AND SIMEN Å. ELLINGSEN<sup>2</sup>

<sup>1,2</sup> Department of Energy and Process Engineering,  
Norwegian University of Science and Technology (NTNU),  
Trondheim, Norway.

<sup>1</sup>e-mail: yan.li@ntnu.no

<sup>2</sup>e-mail : simen.a.ellingsen@ntnu.no

**Key words:** Waves; Shear current; Ring patterns; Ship wakes.

**Abstract:** We present analysis of the effect of a sub-surface shear current with uniform vorticity on hydrodynamic surface waves, showing rich physics and striking results. Due to the non-zero vorticity of the shear flow, standard potential theory solutions are not applicable, and analysis of the wave field is a delicate problem which we tackle by a combination of analytical and computational means. We compute and analyze linearized surface wave solutions to two fundamental problems: initial value problems (ring waves from a localized disturbance) and ship waves. The pattern of ring waves from an initial disturbance is significantly affected by the current, most strikingly so gravity driven waves in deep waters. Next, ship wave patterns in different parameter regimes are presented with special emphasis on the transition from sub-critical to supercritical wakes, a transition governed by a subtle interplay of the effects of the shear current and finite water depth.

## 1 INTRODUCTION

Only very recently has research progress been made on wave-current problems in three dimensions, although a large literature exists on wave-current interactions in two dimensions (see [1]-[4] and references therein). A current other than a uniform one complicates the problem because potential theory, the standard tool in linear wave theory, is not an option once vorticity has been introduced in three dimensions. Of particular interest is the simplest model where the shear flow is assumed to have spatially constant vorticity (a Couette profile). Although not commonly encountered in practice, the uniform vorticity profile has the advantage of allowing analytical progress, being scale independent and facilitating physical transparency since the shear flow is characterized by a single parameter. The author in [5] and [6] successfully obtained a general solution of the classical Cauchy-Poisson problem as well as ship waves by solving linearized Euler and continuity equations. And in [7], an initial value problem with prescribed impulsive pressure is solved for this particular model as well, providing confirmation of the results in [6].

Classically, we have two perspectives when analyzing wave patterns, either a transient one or a stationary one in which the observer follows the travelling wave, applicable for ship waves. In the present paper, we will analyze these two by a variation of external boundary and initial conditions. Through a combination of both analytical and computational approaches, we obtained the corresponding wave patterns. Compared to the various methods which directly

solve governing equations and boundary conditions, our calculations are computationally cheap without loss of accuracy in the linear wave regime. It is also easily parallelizable.

Based on efforts of [5] and [6], the present paper mainly focuses on wave patterns resulting from interactions between wave and shear current with uniform vorticity in three dimensions. We emphasize two fundamental problems: initial value problems and ship waves. Correspondingly, we first derived general solutions for a particular wave-current system. Then, by using an impulsive pressure at  $t=0^+$  and a series of impulsive pressure pulses moving with constant speed, we obtained solutions for the ring wave pattern and ship waves, respectively. We thereafter turn to the numerical method before presenting a brief analysis of the influence of vorticity to the ring patterns both in infinite and shallow waters. Finally, the transition of ship wave patterns between subcritical and supercritical cases in different parameter regimes are demonstrated.

## 2 MATHEMATICAL MODEL AND SOLUTIONS OF SURFACE ELEVATION

### 2.1 Description and coordinate system

In the present paper, incompressible flows are considered, and we assume that viscosity is negligible. In particular we mainly consider the three dimensional wave-current system with uniform depth  $h$ , see Fig. 1. We choose the coordinate system so that the undisturbed water surface is at rest. A shear current with velocity  $U(z)=Sz$  along the  $x$  axis is present underneath the water surface, where  $S$  is the constant vorticity. Although the constant vorticity model allows the use of potential theory in 2D, it is no longer an option in three dimensions [5]. Hence we turn to the continuity and Euler equations as the governing equations, which are

$$\nabla \cdot \mathbf{V} = 0, \quad (1)$$

$$\frac{D\mathbf{V}}{Dt} = -\frac{1}{\rho}\nabla P + \mathbf{g}, \quad (2)$$

in which operator  $\nabla = (\partial/\partial x, \partial/\partial y, \partial/\partial z)$ ,  $\mathbf{V} = \mathbf{V}(x, y, z, t) = (U(z) + u, v, w)$  is the fluid velocity with small velocity perturbations  $u$ ,  $v$  and  $w$ , and total pressure  $P = -\rho gz + p$  with small perturbation  $p$ . The density of the fluid is  $\rho$ , and  $\mathbf{g}$  is the acceleration of gravity pointing in the  $-z$  direction.

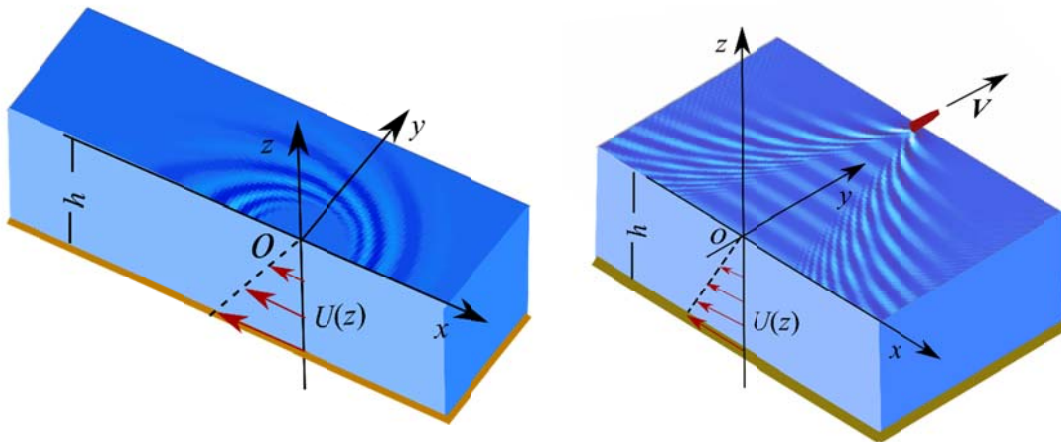


**Figure 1:** Three dimensional wave-current system with uniform depth and coordinate system

The different problems considered differ in their boundary and initial conditions. For the ring waves, we consider a localized initial pressure pulse acting on the free surface for a very short time (using a Dirac delta function) when the surface is at rest. Ship waves may be generated by summing up a continuous series of pressure impulses moving at constant velocity  $V$ ; this procedure is an equivalent alternative to the procedure used in [5] assuming that the waves are stationary as seen from the ship [8]. Generally, for either situation, linearized boundary conditions at the free surface and seabed can be respectively written as

$$\left. \begin{aligned} w|_{z=0} &= \left( \frac{\partial \zeta}{\partial t} + U(z) \frac{\partial \zeta}{\partial x} \right) \Big|_{z=0} \Bigg\} , \\ (P - \rho g \zeta)|_{z=0} &= p_{ext} \end{aligned} \right\} \quad (3)$$

$$w|_{z=-h} = 0 \quad , \quad (4)$$

in which  $\zeta = \zeta(x, y, t)$  is the surface elevation relative to the undisturbed surface, and  $p_{ext}(x, y, t)$  is the external pressure disturbance, which we assume known. For ring waves, we assume that the external pressure is zero for  $t < 0$  and imparts a short impulse on the free surface at  $t=0$  described by a Dirac delta function. Ship waves can be generated by a constant, moving pressure  $-p_{ext}(x, y, t)$ , expressed so that  $p_{ext}(\xi) = p_{ext}(\xi_0)$ , in which  $\xi = \mathbf{x} - Vt$ ,  $\xi_0 = \mathbf{x}$  is the pressure distribution at  $t=0$  and  $\mathbf{x} = (x, y)$  is the position vector. Since our theory is linearized, a continuously moving pressure can be replaced by a continuous series of short impulses integrated over time from  $-\infty$  to  $t$ , and superposition thus allows the formation of ship waves by adding up a continuous train of ring waves.

## 2.2 Solutions of the surface elevation

We follow the same steps as in [5] and [7] and introduce a Fourier transform in the  $xy$  plane to all physical quantities, which are defined

$$\left. \begin{aligned} [u(x, y, z, t), v(x, y, z, t), w(x, y, z, t)] &= \iint \frac{d^2k}{(2\pi)^2} [\tilde{u}(\mathbf{k}, z, t), \tilde{v}(\mathbf{k}, z, t), \tilde{w}(\mathbf{k}, z, t)] e^{i\mathbf{k}\cdot\mathbf{x}} , \\ p(x, y, z, t) &= \iint \frac{d^2k}{(2\pi)^2} \tilde{p}(\mathbf{k}, z, t) e^{i\mathbf{k}\cdot\mathbf{x}} , \\ \zeta(x, y, t) &= \iint \frac{d^2k}{(2\pi)^2} \tilde{\zeta}(\mathbf{k}, t) e^{i\mathbf{k}\cdot\mathbf{x}} , \\ p_{ext}(x, y, t) &= \iint \frac{d^2k}{(2\pi)^2} \tilde{p}_{ext}(\mathbf{k}, t) e^{i\mathbf{k}\cdot\mathbf{x}} , \end{aligned} \right\} \quad (5)$$

in which wave vector  $\mathbf{k} = (k_x, k_y) = (k \cos\theta, k \sin\theta)$ . Applying the Fourier transform to Eq. 1-2 and with the impermeability condition at the seabed, we obtain the general solutions

$$\left. \begin{aligned} \tilde{w} &= kA \sinh k(z+h) \\ \tilde{p}/\rho &= -(\dot{A} + ik_x UA) \cosh k(z+h) + (iSk_x A/k) \sinh k(z+h) \end{aligned} \right\} , \quad (6)$$

In which  $A(\mathbf{k}, t)$  is spatially constant. Substituting Eq. 6 to boundary conditions at the free surface, we obtain

$$\left. \begin{aligned} kA(\mathbf{k}, t) \sinh kh &= \dot{\zeta} \\ -\dot{A} \cosh kh + (iSk_x A/k) \sinh kh - g\zeta &= \tilde{p}_{ext}/\rho \end{aligned} \right\} \quad (7)$$

in which we define  $A_0$  as  $A(\mathbf{k}, 0)$ ,  $\tilde{\zeta}_0$  as  $\tilde{\zeta}(\mathbf{k}, 0)$ , and we used the condition in which current velocity at free surface is zero (otherwise there will be one more term in the linearized kinematic equations).

A Gaussian distribution is used to define the initial pressure impulse at  $t=0$ , which we express as

$$p_I(r, t) = I\delta(t)e^{-(\pi r/a)^2}, \quad (8)$$

wherein  $a$  is the width of the pulse, and

$$\left. \begin{aligned} \tilde{p}_I &= I\delta(t)a^2 e^{-(ka/2\pi)^2} / \pi \\ \int_{-\infty}^{+\infty} \delta(t)dt &= \int_0^{0^+} \delta(t)dt = 1 \end{aligned} \right\}. \quad (9)$$

Referring to [7], by applying Laplace transform to Eq. 6 and substituting the initial impulsive pressure distribution yield the surface displacement

$$\zeta_r / a = \int_0^{2\pi} d\gamma \int_0^{\infty} \frac{-K^2 PI \tanh KH \sin T \sqrt{\Omega_1^2 + \Omega_2^2}}{4\rho\pi^3 \sqrt{\Omega_1^2 + \Omega_2^2}} e^{i(\mathbf{K}\cdot\mathbf{X} - \Omega_1 T) - (K/2\pi)^2} dK \quad (10)$$

in which  $\Omega_1 = -Fr_s \cos \gamma \tanh KH$ ,  $\Omega_1^2 + \Omega_2^2 = (Fr_s \cos \gamma \tanh KH)^2 + K \tanh KH$ , and the non-dimensional quantities are defined in Table 1. In the table, there are three Froude numbers which are defined to examine effects of different parameters: vorticity, ship velocity and water depth.

**Table 1:** Definition of the physical and non-dimensional quantities

Physical quantities	Non-dimensional quantities
$\zeta$	$\zeta/a$
$h$	$H=h/a$
$r(\mathbf{x})$	$X=r/a$ ( $\mathbf{X}=\mathbf{x}/a$ )
$\xi(\zeta)$	$\mathbf{R}=\zeta/a$ ( $R=\zeta/a$ )
$(x, y)$	$(X, Y) = (x/a, y/a)$
$t$	$T = t/\sqrt{a/g}$
$\omega_{1,2}$	$\Omega_{1,2} = \omega_{1,2}\sqrt{a/g}$
$k(\mathbf{k})$	$K=ak$ ( $\mathbf{K}=\mathbf{a}\mathbf{k}$ )
$S$	$Fr_s = S\sqrt{a/g}$
$V$	$Fr_h = V/\sqrt{gh}$ ; $Fr = V/\sqrt{ga}$
$I$	$PI=I/(\rho a\sqrt{ag})$

When simulating the ships or the moving source, we still use the Gaussian pressure impulse but with constant moving speed. Particularly, for different times, we have ring patterns outgoing from the moving source (or the ship), and the continuous ring patterns caused by the moving source will ultimately result in a ship wake as previously described and sketched in Fig. 2. This description of ship waves goes back to Lord Kelvin [9]. However, we will

illustrate in subsequent sections that the wave patterns differ significantly from the classical Kelvin pattern when a shear current is present.

As for the ship wave, we first consider the surface disturbance of time  $t$  caused only by an impulsive pressure at a previous time  $t_0$  ( $t_0 \leq t$ ). The moving source can be expressed as

$$p_{t_0}(\mathbf{x}, t) = p_l(\mathbf{x} - \mathbf{V}t, t - t_0). \quad (11)$$

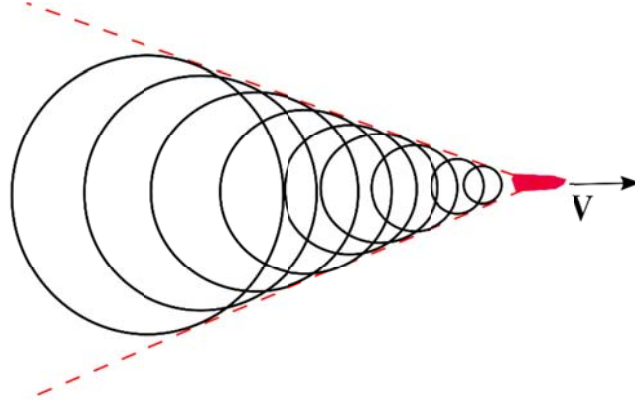


**Figure 2:** ship waves resulted from continuous ring waves

By always considering an origin moving with the source and using previous result, we obtain the surface disturbance

$$\zeta_{t_0} / a = \int_0^{2\pi} d\gamma \int_0^{\infty} \frac{-K^2 PI \tanh KH \sin(T - T_0) \sqrt{\Omega_1^2 + \Omega_2^2}}{4\pi^3 \sqrt{\Omega_1^2 + \Omega_2^2}} \Theta(T - T_0) e^{i[\mathbf{K} \cdot \mathbf{R} + (KFr \cos \gamma - \Omega_1)(T - T_0)] - (K/2\pi)^2} dK, \quad (12)$$

in which  $\Theta$  is the Heaviside step function.

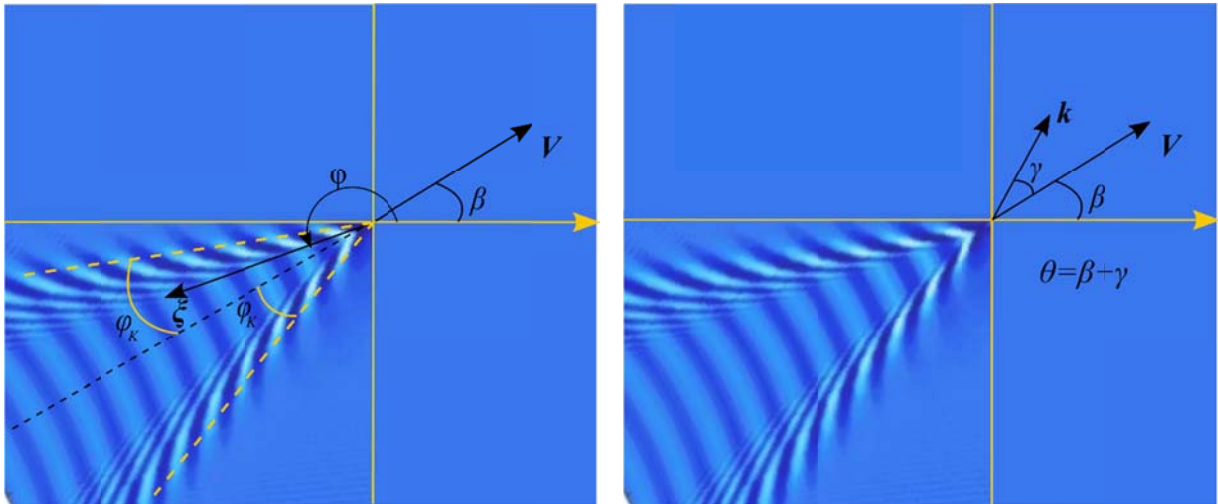


**Figure 3:** Definition of different angles used in this paper

The surface disturbance at time  $t$  can be obtained by integrating contributions from the impulsive pressure disturbance for all of the previous moments, which is expressed as

$$\zeta(t) = \int_{-\infty}^t dt_0 \zeta_{t_0} . \quad (13)$$

Here, we choose the integral range from  $-\infty$  and impose the radiation condition by assuming that all of the physical quantities have increased slowly from zero at  $-\infty$  to its present value. Correspondingly, all of the quantities will be multiplied by the factor  $e^{\varepsilon t}$ , in which  $\varepsilon$  is an infinitesimal positive number and makes sure that Eq. 13 converges. Ultimately, we will get the solution by solving the limit for  $\varepsilon$  approaching to  $0^+$ . It should be noted that we first apply all of the quantities with the form multiplied by term  $e^{\varepsilon t}$  back to the original governing equations, and then follow the whole procedures from Eq. 1-12, thereafter we substitute the new expressions to Eq. 13. This method yields a solution with a stationary phase [8] and we find

$$\zeta / a = \lim_{\varepsilon \rightarrow 0^+} \int_{-\pi}^{\pi} \frac{PI d\gamma}{(2\pi)^2} \int_0^{\infty} \frac{K \tanh KH e^{iK \cdot R - (K/2\pi)^2} dK}{K - \frac{(1 - Fr \cos \gamma \cos(\gamma + \beta)) \tanh KH}{(Fr \cos \gamma)^2} - i\varepsilon \frac{a}{V} \frac{2FrK \cos \gamma - Fr \cos(\gamma + \beta) \tanh KH}{(Fr \cos \gamma)^2}} , \quad (14)$$

in which definitions of  $\beta$  and  $\gamma$  can be seen in Fig.3, which is a brief sketch regarding angles that we use in this paper. Eq. 10 and Eq. 14 are the general solutions with which we will use as the basic foundation of further numerical simulations.

### 2.3 Subcritical and supercritical situations for ship waves

We obtain ship waves in a stationary phase where transient waves make no contribution to the ship wake. Physically, stationary phase refers to a situation where component of the ship velocity in the direction of wave propagation equals the phase velocity, and can be expressed (see [8] and [10])

$$kV \cos \gamma = kc_{\pm}(k, \gamma + \beta) , \quad (15)$$

in which

$$kc_{\pm}(k, \gamma + \beta) = \pm \sqrt{gk \tanh kh + S^2 \cos^2(\gamma + \beta) \tanh^2 kh / 4} - S \cos(\gamma + \beta) \tanh kh / 2 .$$

For a sufficiently fast source a situation may arise when the maximum phase velocity in some directions of wave propagation is insufficient for the wave to keep up with the source. We find that these plane wave components, for which  $V \cos \gamma > c_{\max}(k, \gamma + \beta)$ , make no contribution to the train of waves. A subcritical situation refers to the case when all propagation directions contribute to the far-field waves and the equation  $V \cos \gamma = c(k, \gamma + \beta)$  has a solution  $k(\gamma)$  for every  $\gamma$ .

## 3 NUMERICAL SOLUTIONS AND SPECIAL CASES

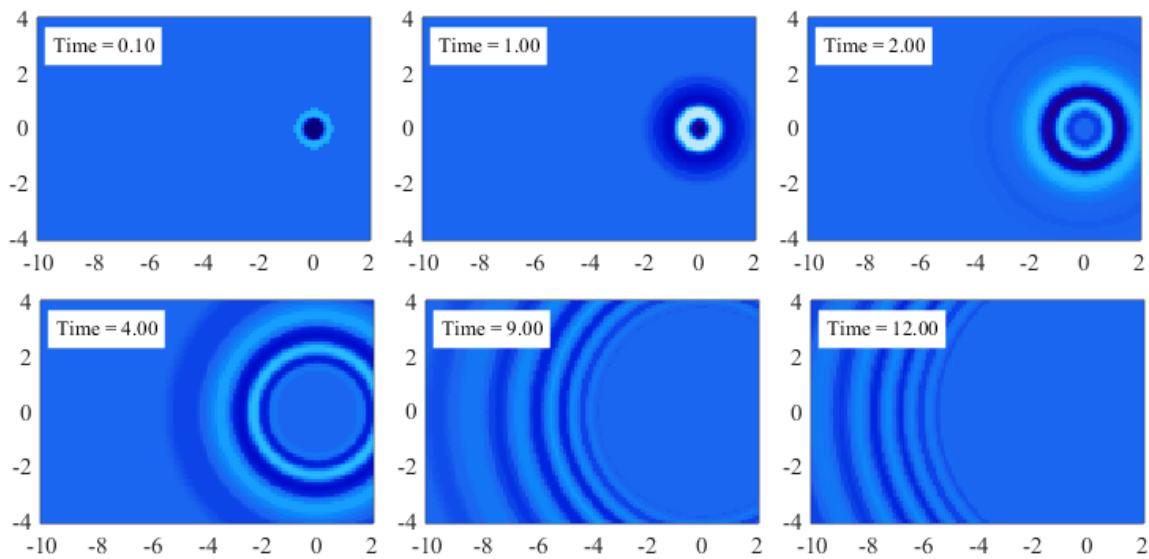
In the previous sections we presented analytical solutions for the particular model presented in this paper. Nevertheless, due to the complicated expressions of the general solution, observing the physical phenomena requires numerical investigation. Hence, numerical evaluation of the integrals in equations (10) and (14) is performed and results are presented below. Note that with these equations, the surface elevation at each point (and similarly, the velocity components in any given point below the surface, not performed here) is calculated

independently of all other points, meaning that parallelization is immediate by simply dividing the grid into segments.

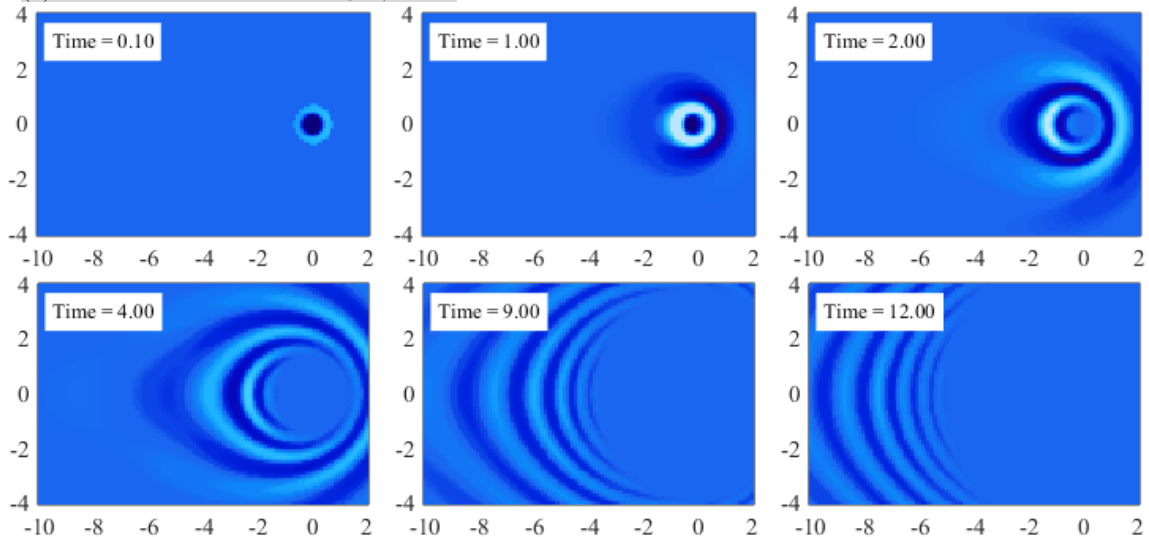
### 3.1 Ring waves

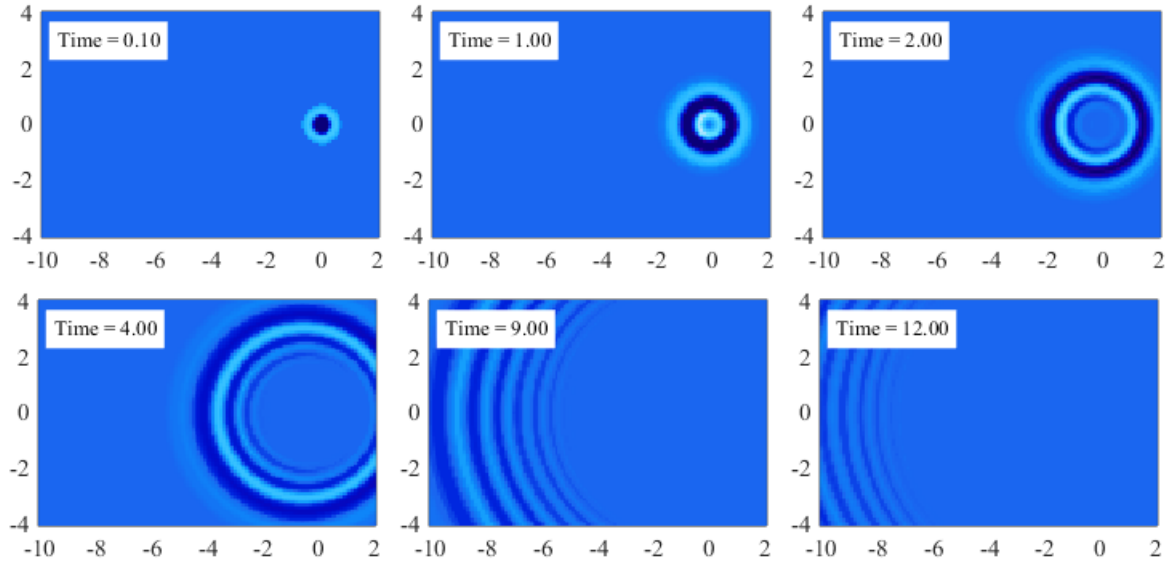
Transient ring waves from an initial pressure impulse are shown in Fig. 4, for 3 different cases: (a)  $Fr_s=0$ ,  $H=20$  (deep water, no shear); (b)  $Fr_s=1$ ,  $H=20$  (deep water, moderate shear); (c)  $Fr_s=1$ ,  $H=0.1$  (shallow water, moderate shear). According to this figure, a perfect ring pattern is shown when there is no shear and there is little effect of moderate shear to waves in shallow water. On the other hand, in deep water the influence of a moderately sheared current to the ring patterns is clear to see, resulting in asymmetric waves from a symmetric pressure input.

(a) Without shear current:  $Fr_s=0$ ,  $H=20$



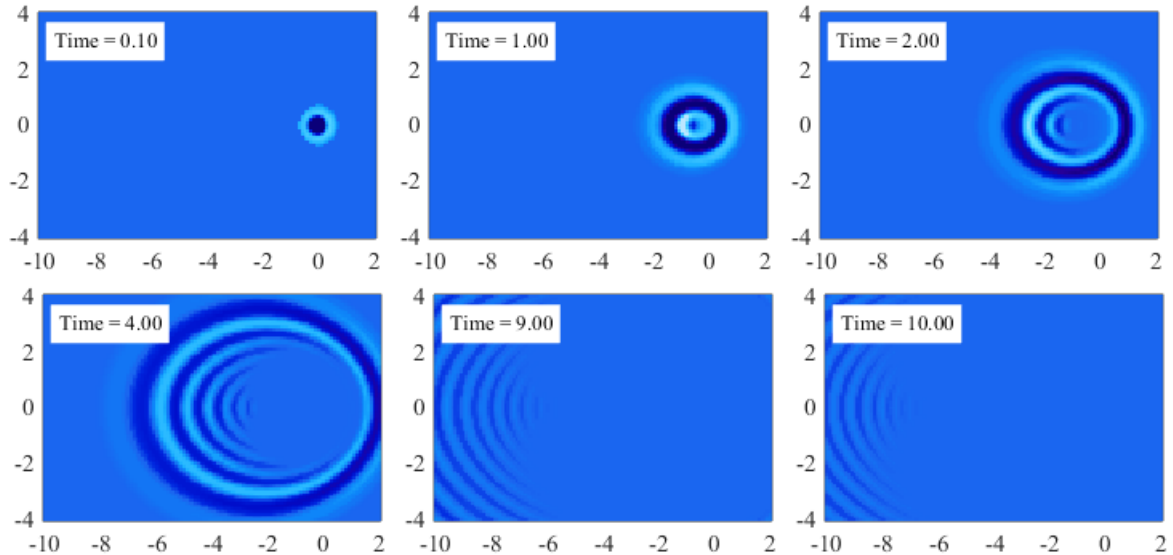
(b) Moderate shear current:  $Fr_s=1$ ,  $H=20$

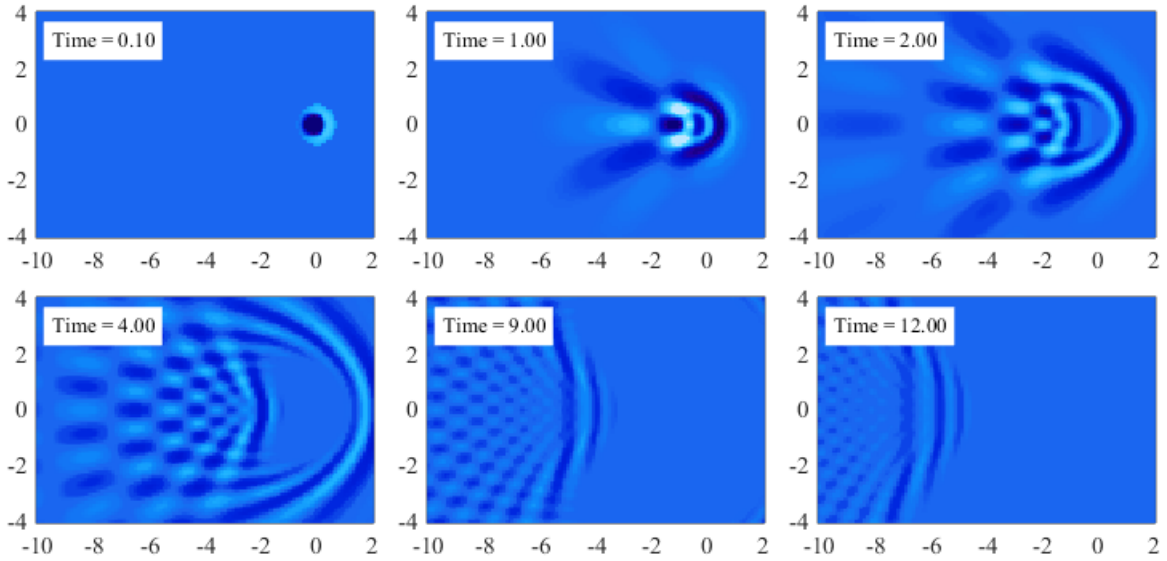


(c) Moderate shear current:  $Fr_s=1, H=0.1$ 

**Figure 4:** Waves in different times with (a)  $Fr_s=0, H=20$ ; (b)  $Fr_s=1, H=20$ ; (c)  $Fr_s=1, H=0.1$ . Contour scaling here and all figures below in Chpt. 3.1 is that areas where  $\zeta(X, Y, T) / a > 0.2 \zeta_{\max}(X, Y, T=0.1) / a$  are white and  $\zeta(X, Y, T) / a < -0.2 \zeta_{\max}(X, Y, T=0.1) / a$  are black, with linear color gradient for amplitudes in between.

We further compared the transient waves of shallow water and deep water with strong shear vorticity,  $Fr_s=4$ , see Fig. 5. It can be seen in Fig. 5 that waves of deep water with strong shear are no longer rings at all, and we can clearly observe effects of vorticity in shallow water in this figure. Clearly the effect of the shear current is much more pronounced in deep waters than in shallow waters. Similar phenomena can also be seen in [5] and [7].

(a) Shallow waters  $H=0.1$ 

(b) Deep waters  $H=20$ **Figure 5:** Waves of deep and shallow waters in different times with strong shear current:  $Fr_s=4$ .

### 3.2 Ship wave patterns

We now turn to ship waves with a shear current in infinite water depth (Fig. 6a) and without shear current in finite water depth (Fig. 6b). As is shown in Fig. 6, Kelvin wake angles (as defined in Ref. [6]) are no longer constant in finite waters even without shear current and reaches to peak for  $Fr_h=1$  – this fact is well known and was reported by Havelock over a century ago [12]. A similar effect is caused by a shear current [6]; even in infinite waters, the Kelvin angle is non-constant but depends on the shear Froude number  $Fr_s$  even though the Froude number  $Fr$  is constant. When the source moves at supercritical velocity, the transverse waves directly behind the source vanish since they are too slow to keep up with the source. The wave patterns showed in Fig. 6b accord well with Ref. [10] which illustrates variation of Kelvin angles with  $Fr_h$  and a critical situation at  $Fr_h=1$  where the Kelvin angle reaches to  $\pi/2$ .

We furthermore illustrate the variation of ship wave patterns between subcritical and supercritical cases with shear current in waters of different depth. Fig. 7 shows this phenomenon, which presents ship wave patterns of different shear vorticities in both finite and infinite waters. In the figure, the shear is made gradually stronger, and a transition from subcritical to supercritical or *vice versa* is observed. Wave patterns are more complicated in a finite water than in an infinite water because of the nontrivial interplay between shear and finite depth. When the angle between ship motion and current changes, waves can experience a transition from subcritical to supercritical as well as from supercritical to subcritical in finite water cases, the former of which is showed with  $\beta=30^\circ$ , and latter of which is with  $\beta=150^\circ$ . However, a supercritical to subcritical transition due to increasing  $Fr_s$  will never occur for infinite waters. A more detailed explanation for this phenomenon is given in [8] (some preliminary conclusions are found in [10]) where a general criticality condition as a function of  $Fr_s$ ,  $Fr_h$  and  $\beta$  is given.

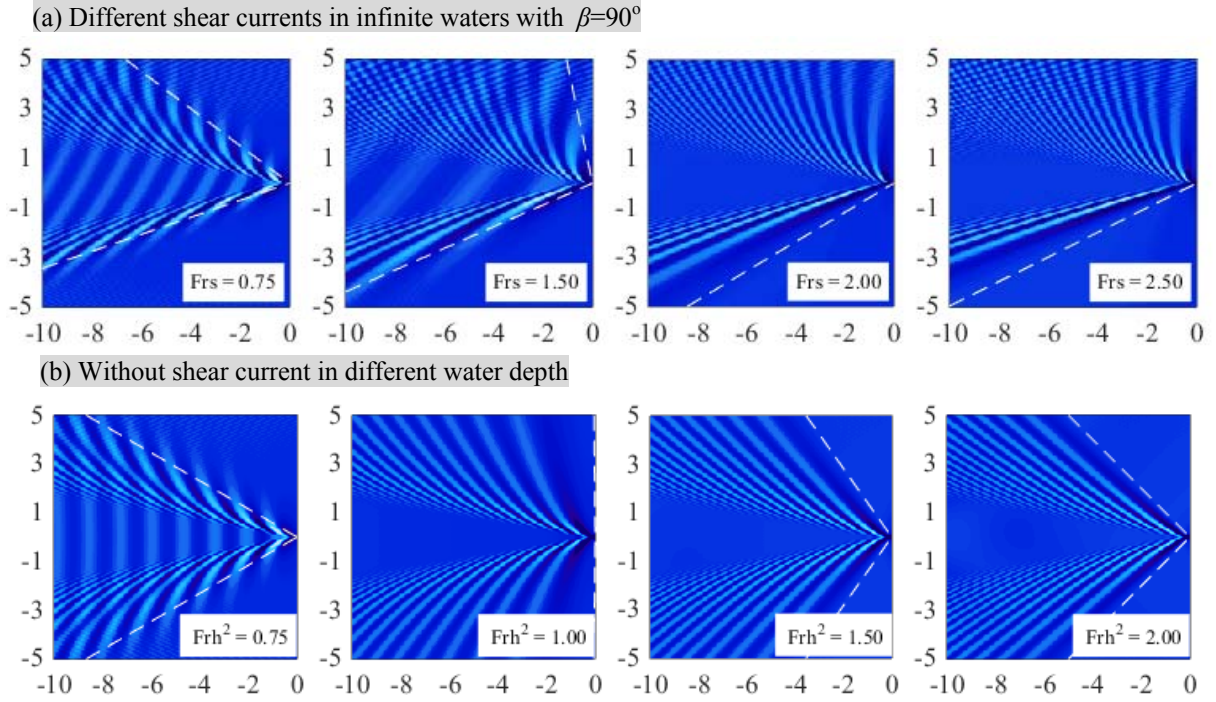
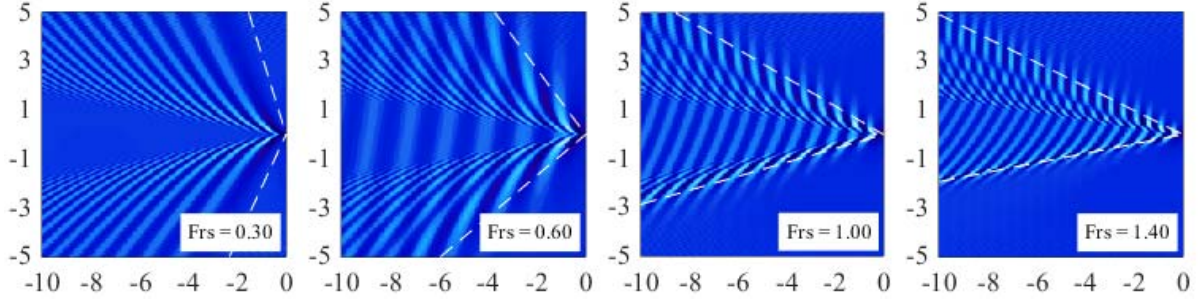


**Figure 6:** Ship waves with  $Fr=0.8$ . In this figure and all figures below in Chpt. 3.2, red dashed lines represent the Kelvin angles as defined in Ref. [6], axes are in units of  $\lambda_0=2\pi a Fr^2$ , and relief shading from light to dark has scaled by corresponding maximum amplitude of surface displacement, areas where  $\zeta > 0.4 \zeta_{max}$  are light and  $\zeta < -0.3 \zeta_{max}$  are dark, with linear gradient color for amplitude in between.

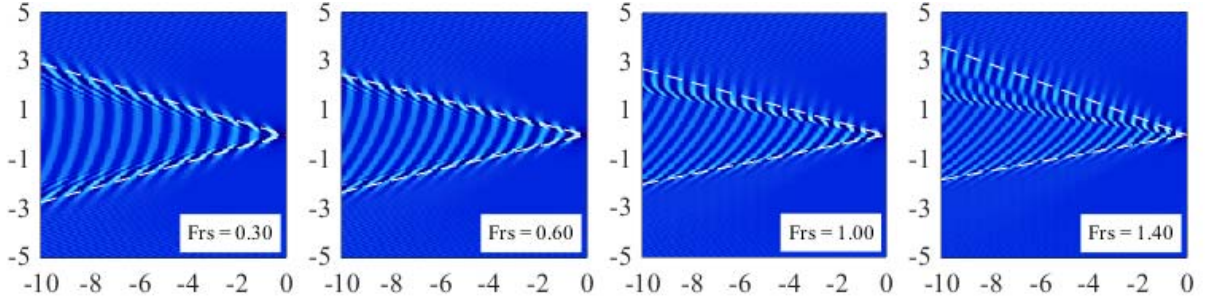
#### 4 CONCLUSIONS

In the present paper, wave patterns were calculated for two fundamental problems in the presence of a shear current with constant vorticity — an initial value problem and a stationary phase problem caused by a moving object. We first derive analytical results which are subsequently subjected to numerical computations. For an initial problem of ring waves created by a short pressure impulse, we demonstrated how the shear affects surface waves more strongly in deep waters (compared to size of disturbance) than in shallow waters. In the former case the ring waves can be distorted to such an extent that they are no longer ring shaped at all. As for ship waves, we illustrated that transitions of the wave pattern both from a supercritical to subcritical and from a subcritical to supercritical can occur in finite waters when increasing the shear vorticity. Nevertheless, only subcritical to supercritical can happen in deep waters. Thus a subtle interplay of water depth and shear was likewise shown to affect the ship waves.

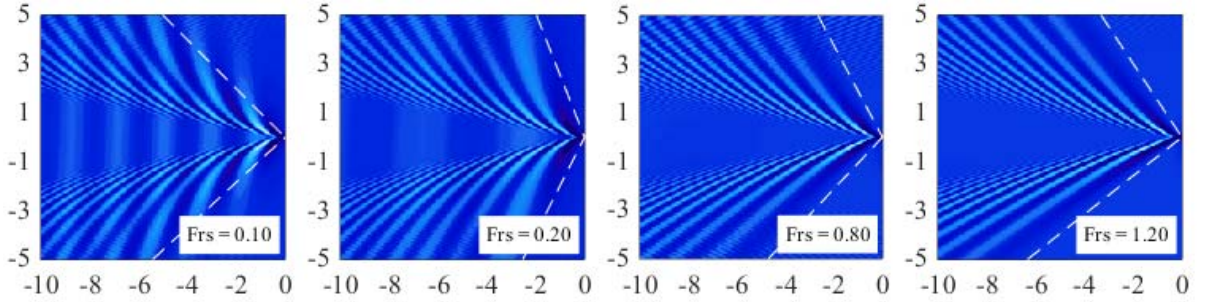
Finite water depth with  $Fr_h^2=1.4$  and  $\beta=150^\circ$ . Critical value at  $Fr_s \approx 0.48$ . (Supercritical to subcritical)



Infinite water depth:  $\beta=150^\circ$ ,  $Fr_h^2=0$ . Critical value at  $Fr_s \approx 15$ . (All panels subcritical)



Finite water depth with  $Fr_h^2=0.8$  and  $\beta=30^\circ$ . Critical value at  $Fr_s \approx 0.23$ . (Subcritical to supercritical)



Infinite water depth:  $\beta=30^\circ$ . Critical value at  $Fr_s \approx 1.07$ . (Subcritical to supercritical)

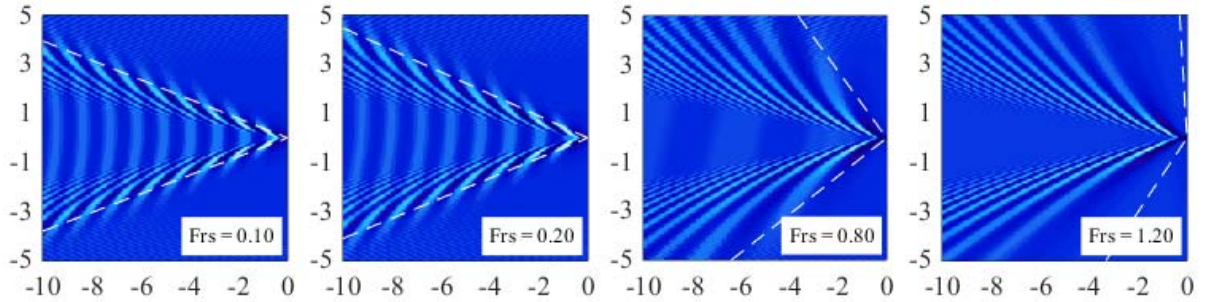


**Figure 7:** Ship wave patterns varying from supercritical to subcritical (or from subcritical to supercritical) for different situations with  $Fr=0.8$ .

## REFERENCES

- [1] Booker, J. R. & Bretherton, F. P., The critical layer for internal gravity waves in a shear

- flow, *Journal of Fluid Mechanics*, vol. 27, pp. 513-539, (1967).
- [2] Peregrine, D. H. Interaction of water waves and currents. *Advances in Applied Mechanics*, vol 16, pp. 9-117, (1976).
- [3] Teles da Silva, A. F. & Peregrine, D. H., Steep, steady surface waves on water of finite depth with constant vorticity. *Journal of Fluid Mechanics*, vol. 195, pp. 281-302, (1988).
- [4] Ellingsen, S. Å. & Brevik, I. How linear surface waves are affected by a current with constant vorticity. *European Journal of Physics*, vol. 35, 025005, (2014).
- [5] Ellingsen, S. Å. Initial Surface disturbance on a shear current: the Cauchy-Poisson problem with a twist. *Physics of Fluids*, vol. 26, 082104, (2014).
- [6] Ellingsen, S. Å. Ship waves in the presence of uniform vorticity. *Journal of Fluid Mechanics*, vol. 72, R2, (2014b).
- [7] Li, Y. & Ellingsen, S. Å. Initial value problems for water waves in the presence of a shear current. *Proceedings of the Twenty-fifth International Ocean and Polar Engineering Conference (ISOPE)*, pp. 543-549, (2015).
- [8] Li, Y. & Ellingsen, S. Å. Ship waves on uniform shear current: wave resistance and finite water depth. *Manuscript under review*.
- [9] Sir W. Thomson (Lord Kelvin). On ship waves. *Proc. Inst. Mech. Eng.*, Vol. 38, pp. 409-434, (1887).
- [10] Ellingsen, S. Å & Li, Y. Ship waves at finite depth in the presence of uniform vorticity, *Proceedings of 30<sup>th</sup> International Water Waves and Floating Bodies/ IWWWFB*, (2015).
- [11] Darmon, A., Benzaquen, M, & E. Raphaël. Kelvin wake pattern at large Froude numbers. *Journal of Fluid Mechanics*, vol. 738, R3, (2014).
- [12] Havelock, T. H. The propagation of groups of waves in dispersive media, with application to waves on water produced by a travelling disturbance. *Proceedings of the Royal Society of London A*, vol. 81, pp. 398—430 (1909).